Mechanism of One-Way Traffic of Hexameric Phi29 DNA Packaging Motor with Four Electropositive Relaying Layers Facilitating Antiparallel Revolution

Zhengyi Zhao,[†] Emil Khisamutdinov,[†] Chad Schwartz,[†] and Peixuan Guo*

Nanobiotechnology Center, Markey Cancer Center, and Department of Pharmaceutical Sciences, College of Pharmacy, University of Kentucky, Lexington, Kentucky 40536, United States. [†]These authors contributed equally to this work.

ABSTRACT The importance of nanomotors in nanotechnology is akin to that of mechanical engines to daily life. The AAA+ superfamily is a class of nanomotors performing various functions. Their hexagonal arrangement facilitates bottom-up assembly for stable structures. The bacteriophage phi29 DNA translocation motor contains three coaxial rings: a dodecamer channel, a hexameric ATPase ring, and a hexameric pRNA ring. The viral DNA packaging motor has been believed to be a rotational machine. However, we discovered a revolution mechanism without rotation. By analogy, the earth revolves around the sun while rotating on its own axis. One-way traffic of dsDNA translocation is facilitated by five factors: (1) ATPase changes its conformation to revolve dsDNA within a hexameric channel in one direction; (2) the 30° tilt of the channel subunits causes an antiparallel arrangement between two helices of dsDNA and channel wall to advance one-way translocation; (3) unidirectional flow property of the internal channel loops serves as a ratchet valve to prevent reversal; (4) 5′—3′ single-direction movement of one DNA strand along the channel wall ensures single direction; and (5) four electropositive layers interact with one strand of the electronegative dsDNA phosphate backbone, resulting in four relaying transitional pauses during translocation. The discovery of a riding system along one strand provides a motion nanosystem for cargo transportation and a tool for studying force generation without coiling, friction, and torque. The revolution of dsDNA among 12 subunits offers a series of recognition sites on the DNA backbone to provide additional spatial variables for nucleotide discrimination for sensing applications.

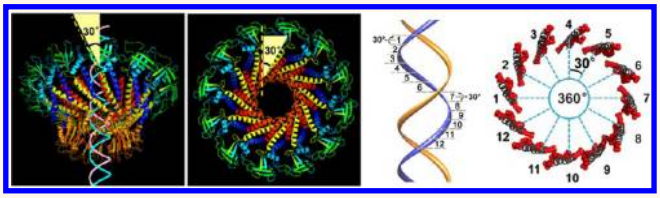

KEYWORDS: bionanomotor · AAA+ ATPase superfamily · one-way traffic mechanism · DNA packaging · virus assembly · bionanotechnology

Biological nanomotors are ubiquitous. The AAA+ (ATPases Associated with diverse cellular Activities) superfamily of proteins is a class of biological nanomotors with a wide range of functions, including DNA translocation, tracking, and riding.[1−8] These motors show great potential for use in nanotechnological applications and have proven to be as important to nanotechnology as mechanical motors are to daily life. Most members of this family fold into hexameric arrangements;[1,2,4,5,7,9−11] since all angles are factors of 360°, this hexagonal structure with an interior angle of 120° and external angle of 60° could facilitate bottom-up assembly or simple fabrication to produce a stable structure or arrays. Despite their functional diversity, the common characteristic of these motors is their ability to convert chemical energy obtained from the hydrolysis of the γ-phosphate bond of ATP into a mechanical force and physical motion, a process usually involving a shift in entropy and a change in conformation of the motor building block. This change of conformation generates a gain or loss of affinity for its substrate, leading to mechanical movement by breaking contacts between macromolecules; assembly or disassembly of the complex; induction of substrate unfolding; and promotion of translocation of DNA, RNA, proteins, or other macromolecules. In a cellular environment, these activities underlie processes critical to DNA repair, replication,

* Address correspondence to peixuan.guo@uky.edu.

Received for review January 18, 2013 and accepted March 20, 2013.

Published online 10.1021/nn4002775

recombination, chromosome segregation, DNA/RNA transportation, and many others.[12,13]

In both prokaryotic and eukaryotic cells, DNA needs to be transported from one cellular compartment to another. During replication, dsDNA viruses translocate their genomic DNA into preformed protein shells, termed procapsids (for review, see refs 14−17). This entropically unfavorable process is accomplished by a nanomotor that uses ATP as an energy source.[18−21] The dsDNA translocation motor consists of a protein channel and two molecules that carry out its activities:[22−24] an ATPase[18,25−31] and, in the phi29 bacteriophage, a hexameric RNA ring. Our discovery 25 years ago proved that the larger molecule serves as part of the ATPase complex used in energy production, and the smaller one is responsible for binding to the dsDNA substrate.[18,23] This notion has now become well-established.[14−17] The connector contains a central channel encircled by 12 copies of the protein gp10 that serve as a pathway for dsDNA translocation.[32,33] This dodecameric connector protein has shown great potential in nanotechnology and nanomedicine applications because of its ability to form peptide-mediated,[34,35] as well as nucleotide-mediated,[36] self-assembled nanoparticles. Also advantageous is the realization that it can be constructed into multilayers[37,38] and single-layer patterned arrays,[39] and it has a high sensitivity for real-time sensing of nucleotides and single chemicals.[40,41]

In 1978, an attractive model with a five-fold/six-fold rotation mechanism for bacteriophage dsDNA packaging was proposed.[42] Since then, it has been popularly believed that viral DNA translocation motors are rotating machines.[33,42,43] Many other intriguing translocation models have subsequently been proposed for the motor of dsDNA viruses.[17,44−47] The most well-studied system is the bacteriophage phi29 DNA translocation motor, constructed in 1986.[48] In 1987, an RNA component was discovered on the translocation motor,[22] and subsequently, in 1998, this RNA particle was determined to exist as a hexameric ring[23,49] (featured by *Cell*[50]). On the basis of this structure, it was proposed that the mechanism of phi29 viral DNA translocation is similar to that used by other hexameric DNA tracking motors of the AAA+ family.[23] This notion has induced fervent debates concerning whether the motor is a hexamer or a pentamer.

In a rotational model, at least one of the three coaxial rings in the translocation motor, or the dsDNA itself, should rotate during dsDNA translocation. Several published data have confirmed that none of the motor components, including the connector, the dsDNA, and the ATPase gp16, rotate during DNA translocation.[24,51−53] For example, studies combining the methods of single-molecule force spectroscopy with polarization-sensitive single-molecule fluorescence optical trapping[52] proved that the connector does not rotate. This was further supported by an experiment in which the connector was covalently linked to the capsid protein of a procapsid, making rotation of the connector within the procapsid impossible.[51,52,54] When the connector and the procapsid were fused to each other, rotation of the connector within the procapsid was not possible. However, the motors were still active in translocating dsDNA and producing active viruses, implying that connector rotation is not necessary for DNA translocation. Our single-molecule studies using beads tethered to the end of dsDNA have revealed that dsDNA was still packaged into the procapsid even with such tethering.[24,53] The results raised a question regarding the operation of the phi29 DNA translocation motor since it does not follow the rotational mechanism. Thus, this seemingly simple rotary machine was still a mystery. Although the application of this motor in nanotechnology has been attempted,[34−41] demonstration of its potential has been diminished by opposing literature regarding the motor mechanism. Elucidation of its operating mechanism is essential for the field of nanobiotechnology.

Recently, we discovered a novel mechanism for the viral DNA translocation motor: the motor uses a revolution mechanism without involving the rotation of any of the motor components or coiling of dsDNA.[55] The motor contains six copies of ATPase gp16.[56] During DNA translocation, dsDNA revolves unidirectionally along the dodecameric channel wall (see Supporting Information). ATP binding to one ATPase subunit stimulates the ATPase to adapt a conformation with a high affinity to bind dsDNA. ATP hydrolysis induces a new conformation with a lower affinity for dsDNA, thus pushing dsDNA away and transferring it to an adjacent subunit by a power stroke. One ATP is hydrolyzed in each one of the six transitional steps, and six ATPs are consumed in one helical turn of 360°. As demonstrated with Hill constant determination, binomial assay, cooperativity and sequential analysis, transition of the same dsDNA chain along the channel wall, but at a location 60° different from the last contact, urges dsDNA to move forward 1.75 base pairs with each step (10.5 bp/turn ÷ 6ATP = 1.75 bp/ATP). Through evolution, nature has conceived a clever revolution machine to translocate the DNA double helix while avoiding the difficulties associated with DNA supercoiling, friction, and torque force during rotation. The revolution without rotation model could resolve a big conundrum troubling the past 35 years of painstaking investigation of the mechanism of these DNA packaging motors. With the revolution mechanism, dsDNA continues to advance without the need for rotation! The one-way traffic property of the motor has previously been reported,[57] but the mechanism has remained enigmatic. In this paper, we elucidate how the motor components coordinate to revolve the dsDNA, ensure a one-way traffic mechanism, and continuously advance dsDNA without reversing.

RESULTS AND DISCUSSION

Unique Structure of Three Coaxial Hexameric Rings of Phi29 Motor Ensure One-Way Traffic. The phi29 DNA translocation motor is composed of three coaxial rings (Figure 1): a hexameric ATPase ring that serves as the force generating machine, a dodecameric channel that serves as a path for dsDNA,[32,33,57] and a hexameric RNA ring that connects and gears the connector and the ATPase.[58−60] The one-way traffic phenomenon has been verified by voltage ramping, electrode polarity switching,[57] and sedimentation force assessment.[57] However, the mechanism for controlling the one-way translocation had not been elucidated.

Most recently, we discovered that the motor uses a revolution instead of a rotation mechanism,[55] which greatly promotes our understanding of this one-way property. We found that the motor uses five different modules to control the direction of translocation: (1) the motor ATPase plays a major role in producing energy to push the dsDNA to advance toward the connector *via* dsDNA revolution within the channel;[55,56] (2) the 30° tilt and the antiparallel arrangement between the two helixes of dsDNA and the connector channel subunit enhance the translocation of dsDNA in a single direction; (3) the unidirectional flow property of the internal channel loops serves as a ratchet valve to prevent reversal of dsDNA; (4) the 5′−3′ single-direction movement of one strand of dsDNA along the phi29 motor connector channel wall ensures a unidirectional motion; and (5) four relaying lysine layers interact with a single strand of the dsDNA phosphate backbone, resulting in four steps of transition and pausing during dsDNA translocation.

ATPase Pushes the Double-Stranded DNA To Revolve in One Direction along Its Hexameric Channel. The ATPase gp16 controls the one-way traffic by two mechanisms. The first mechanism is the "push through a one-way valve" mechanism,[16,57,61,62] and the second one is the revolution of dsDNA along the dodecameric channel wall.[56]

The following is the force generation mechanism from the ATPase gp16. ATPase exists in a hexameric form (Figure 1B).[56] The binding of ATP to one gp16 subunit stimulates it to adapt to a conformation with a higher affinity for dsDNA, while ATP hydrolysis forces gp16 to assume a new conformation with a lower affinity for dsDNA, thus pushing dsDNA away from one subunit and transferring it to an adjacent subunit (Figure 2).[55,62] Such physical transition pushes the DNA through the one-way valve channel, urging the dsDNA to advance inward to enter the procapsid but not in reverse. This conclusion was supported by gel shift assays. In the absence of γ-S-ATP, a nonhydrolyzable derivative of ATP, the binding of gp16 to DNA is weak (Figure 3, lane 3). However, after the addition of γ-S-ATP, the binding efficiency of gp16 to DNA increased significantly (Figure 3, lane 4) since the complex is frozen by the nonhydrolyzable ATP. This evidence supports the above conclusion that ATP induces a conformational change in gp16 that causes it to assume a high affinity conformation for dsDNA binding. More significantly, when ATP was added to the gp16−γ-S-ATP−dsDNA complex, rapid ATP hydrolysis was observed[62] and gp16 dissociated from the dsDNA. This indicates that, after hydrolysis, gp16 undergoes a further conformational change that produces an external force against the dsDNA and pushes the substrate away from the motor complex by a power stroke. This also agrees with the result shown in Figure 3, lane 5, providing evidence for the existence of two ATPase conformations under different conditions with various ATP concentrations.

The second mechanism of one-way traffic control is directed *via* dsDNA revolution through the gp16 hexameric ring in one direction (Figure 2). During DNA translocation, only one strand of the dsDNA interacts with the dodecameric channel wall (see Supporting Information), and neither the dsDNA nor the hexameric ATPase rotates (Figure 2). One ATP is hydrolyzed in each transitional step, and six ATPs are consumed for

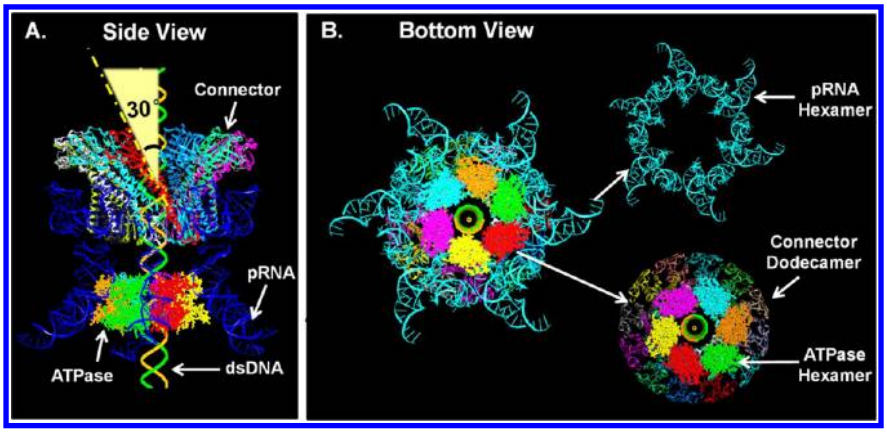

Figure 1. Illustration of the phi29 DNA packaging motor structure. Side view (A) and bottom view (B). The 30° tilt of the helix of the connector subunit and its antiparallelism with the dsDNA helix is depicted (A). The three coaxial rings: pRNA hexamer, ATPase hexamer, and connector dodecamer in the phi29 DNA packaging motor are depicted (B).

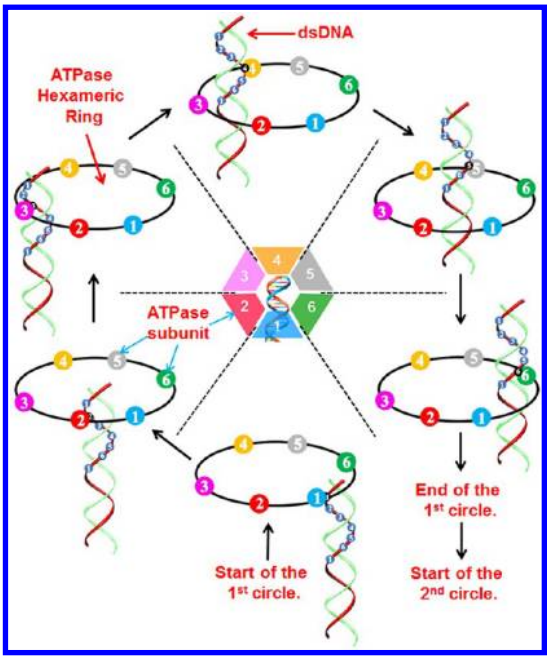

Figure 2. Schematic of the revolution mechanism employed in translocating genomic DNA. The binding of ATP to one subunit stimulates gp16 to adapt to a conformation with a higher affinity for dsDNA. ATP hydrolysis forces gp16 to assume a new conformation with a lower affinity for dsDNA, thus pushing dsDNA away from the subunit and transferring it to an adjacent subunit. Rotation of the hexameric ring or the dsDNA is not required since the dsDNA chain is transferred from one point on the phosphate backbone to another. For the revolution motion of genomic DNA along the 12 subunit channel wall, please see Supporting Information.

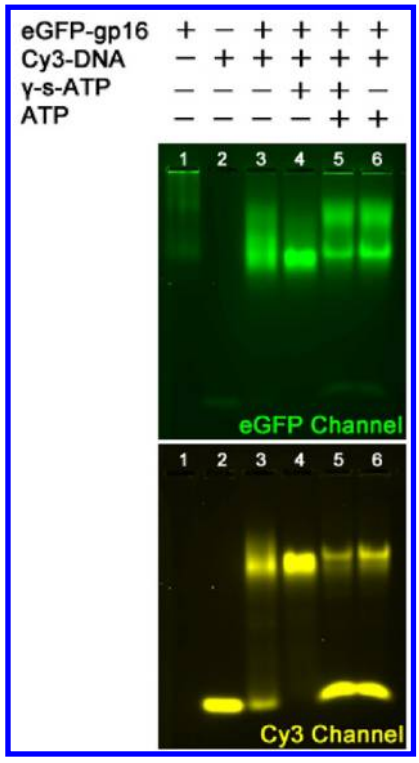

Figure 3. EMSA of eGFP-gp16 configurations with short Cy3-dsDNA and ATP or γ-S-ATP. The GFP channel shows migration of the ATPase, and the Cy3 channel shows the migration of the dsDNA. The eGFP channel lane 5 clearly shows two distinct bands of gp16 after addition of ATP, indicating the presence of two conformations of gp16.

one helical turn of 360° or 10.5 bp (base pairs). As demonstrated with Hill constant determination, binomial assay, cooperativity, and sequential analysis, transition of the same dsDNA chain along the channel wall, but at a location 60° different from the last contact, urges dsDNA to revolve forward with a single orientation at 1.75 bp (10.5 bp per turn ÷ 6 ATP = 1.75 bp/ATP).[51,63]

The 30° Tilting of Channel Subunits Causes an Antiparallel Arrangement between Two Helices Resulting in Revolution in a Single Direction. A cone-shaped central channel is encircled by 12 copies of the protein connector subunit gp10 and serves as a pathway for dsDNA translocation.[32,33] The wider C-terminal end, 13.6 nm in diameter, is buried inside the procapsid. The narrower N-terminal end is 3.6 nm in diameter and allows dsDNA to enter. The connector is a one-way valve that only allows dsDNA to move into the procapsid unidirectionally,[41] as verified by voltage ramping, electrode polarity switching, and sedimentation force assessment.[57] All 12 gp10 subunits are tilted at a 30° angle and encircle the channel in a configuration that runs antiparallel to the dsDNA helix residing in the channel. The antiparallel arrangement between the two helices of the connector subunit, and the helix of the dsDNA, can be visualized in an external view (Figure 4A), with dsDNA potentially making contact at each connector subunit (Figure 4).

The antiparallelism exhibited by the helices argues against a bolt and screw rotation model since a screw thread and the corresponding whorl should match. The 30° tilt of the subunits matches perfectly with the 30° transitions that the dsDNA helix exhibits during revolution (360° ÷ 12 = 30°). In each step of revolution that moves the dsDNA to the next subunit, the dsDNA physically moves to a second point on the channel wall, keeping a 30° angle between the two segments of the DNA strand (Figure 4). This structural arrangement enables the dsDNA to touch each of the 12 connector subunits in 12 discrete steps of 30° transitions for each helical pitch (Figure 4). Nature has created and evolved a clever machine that advances dsDNA in a single direction while avoiding the difficulties associated with rotation, such as DNA supercoiling, as seen in many other processes. For reference, the Earth *rotates* around its own axis every day, but *revolves* around the sun every 365 days.

Unidirectional Flow of the Internal Channel Loops Provides a Vector Force as a Ratchet Preventing DNA Reversal. The phi29 connector allows dsDNA to translocate from its N-terminal (narrower end) to its C-terminal (wider end).[41] In our most recent findings, like other ion channels that play a critical role in regulating ions in and out of membranes, the phi29 motor channel gates in three discrete steps in response to high voltage or

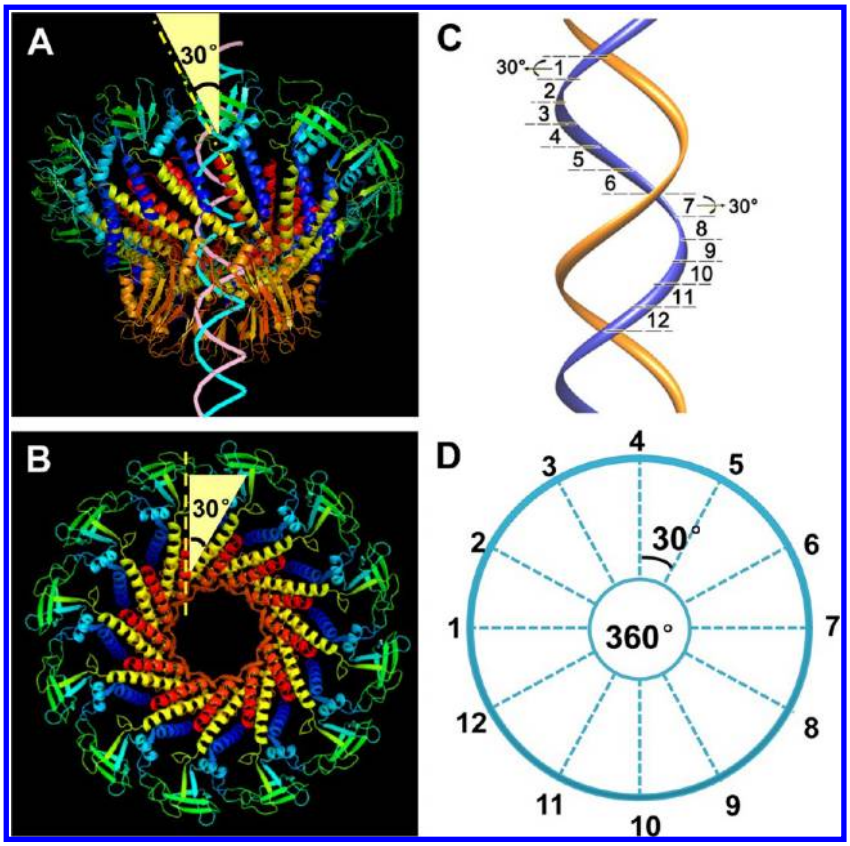

Figure 4. Illustration showing the antiparallel configuration between connector subunit and DNA helix. External view (A) and internal view (B) of the antiparallel configuration of connector and DNA as dsDNA revolves through the connector. One-twelfth of a dsDNA helix is 30° (C), which is the angle dsDNA revolves to advance between two adjacent connector subunits (D). The contact at every 30° for twelve 30° transitions resulted in translocation of one helical turn of the dsDNA through the connector (B).

ligand binding.[57,64] We have constructed a mutant connector in which the internal loops, which have been believed to play a role in DNA packaging, with residues 229−246[33,61] were deleted. The viral assembling activities of procapsids bearing this mutant connector were assessed by *in vitro* virion assembly. It was found that procapsids with the loop-deleted connector failed to produce any virions, as compared to wild-type procapsids in which the assembly activity was about 1×10^8 pfu/mL (plaque forming units per milliliter) (Figure 5B). Other findings from our lab and other groups have revealed that the channel loops play a critical role in the one-way traffic mechanism of dsDNA and that the packaged dsDNA reverses and slides out after being packaged into the mutant procapsid.[17,61,64−66] The channel loops may act as a clamp during DNA translocation and prevent the DNA from sliding out, supporting the push through a one-way valve model in which the direction of DNA migration is regulated by the loops inside the channel[61] (Figure 5A).

The application of single-pore conductance assay revealed a one-way traffic of normal connector channel and two-way traffic of internal channel loop-deleted connector (Figure 6). DNA traffic was probed by applying a ramping potential (Figure 6, left panel) and by switching the voltage polarity (Figure 6, right panel) that crossed the membrane. Due to the negative charge of the phosphate backbone, DNA migrates from the negative toward the positive electrode. In the presence of DNA in both *cis*- and *trans*-chambers under a ramping potential, DNA translocated *via* the single-channel BLM only at the negative potential when channel entrance (the narrow end which locates outside the procapsid) faced the negative electrode (Figure 6A). On the contrary, DNA translocation was observed only at the positive potential when the channel turned upside down (Figure 6B). Furthermore, in the presence of DNA in both *cis*- and *trans*-chambers under a constant voltage, DNA translocation *via* the single channel could be turned on and off depending on the polarity of the voltage[57] (Figure 6E). This correspondence to polarity switching was dependent upon the orientation of the connector in the BLM, which was determined by nanogold blocking assay.[57] When no DNA translocation was observed under negative potential, switching the voltage to positive potential resulted in DNA translocation (Figure 6E) and *vice versa*. The results strongly support that dsDNA can only pass through the wild-type connector channel in one direction. When the internal loops of the connector were deleted, the two-way traffic of

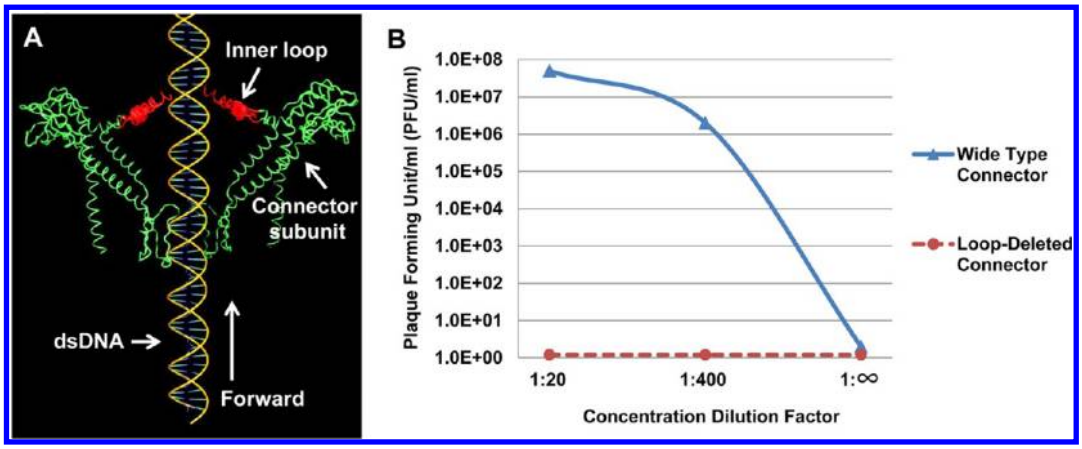

Figure 5. Illustration showing the influence of the flexible inner channel loops on DNA movement and virion assembly assay using procapsid harboring connectors with internal loop deletion. (A) Flexible loop within the connector channel functions to interact with the DNA, facilitating the DNA to move forward, but blocking the reversal of DNA during DNA packaging. (B) Two dilution factors of wild-type procapsid show high virion assembly activity (~10^7 pfu/mL), while procapsids harboring the connectors with internal loops deleted are of a very low virion assembly activity. The loops are assumed to facilitate the forward movement of DNA and enhance the DNA one-way traffic mechanism but not the reverse.

DNA was observed using both scanning potential (Figure 6C) and polarity switching (Figure 6F). So far, the two-way traffic of DNA has not been detectable for the wild-type connector under the current experimental conditions.[67] In summary, the conductance assay with specific mutant connectors demonstrated that the internal flexible loops are essential for the one-way traffic of the motor. Together with the finding that procapsids harboring modified connectors with internal channel loop mutation or deletion lose the capability to retain DNA after packaging,[65] as well as our finding that the procapsids harboring modified connectors with internal channel loop deletion decrease the virion assembly efficiency (Figure 5B), we concluded that the internal flexible loops play a key role in the one-way traffic property of viral DNA packaging motors during DNA translocation.

The 5′—3′ Single-Direction Movement of One DNA Strand along the Channel Wall Ensures Unidirectional Motion. Our extensive investigations into data modeling and literature have led to the following conclusions: the motor only contacts one strand, not both, of the dsDNA in the 5′ to 3′ direction in order to revolve along the connector channel.[47] While single-stranded DNA cannot be packaged, dsDNA with the 3′-end extended can revolve along the channel one helical turn of 10.5 bp. This notion has been based upon the revolution (but not the rotation) model and agrees with our studies on phi29 DNA packaging of phi29 genomic DNA containing single-stranded gaps.[68] The gap-containing dsDNA were produced *in vitro*, and the DNA packaging function was assayed in agarose gel electrophoresis using the defined *in vitro* phi29 assembly system.[69,70] We found that phi29 DNA with single-stranded gaps was not packaged at full genome length. Because of such, we created two gaps: one at the left end (5883 bp) and one at the right end (14 421 bp) of the phi29 DNA genome. Only the 5.9 kb DNA fragment between the left end of the genome and the first gap was packaged.[68] The right end fragment was not packaged. The result suggests that a single-stranded gap in the DNA is a structural alteration that can cause the packaging motor to stop, and that the packaging direction is from 5′ to 3′ since the phi29 packaged the left end of the genome first. Our model is supported by the finding by Black and co-workers who reported that a 3′ single-stranded overhang was packaged under conditions extending from the 100 bp duplex.[71] A 3′ extension up to 12 bases did not inhibit translocation, whereas 20 or more bases significantly blocked the T4 motor in DNA packaging. The 20 base gap was consistently found to be vulnerable, whether it was at the 3′ end or in the middle of the DNA strand.[71] These results support the notion that the motor can revolve one complete turn of 360° with a single-stranded structure and that dsDNA revolves along the motor using a single strand in the 5′ to 3′ direction. The data are also supported by experimental data involving optical tweezers showing that dsDNA is processed by having contact with an unknown component on one strand of DNA in the 5′ to 3′ direction; the modification of phi29 DNA in the 5′ to 3′ direction stopped dsDNA packaging;[47] as well, that modification with 10 bases is tolerable, but 11 bases is not.[47]

Four Electropositive Relaying Layers Interact with the Electronegative DNA Backbone, Resulting in Four Steps of Transitional Pauses. Connector crystal analysis[33] has revealed that the dominantly negatively charged phi29 connector interior channel surface is decorated with 48 positively charged lysine residues, existing as four relaying 12 lysine rings derived from the 12 protein subunits that enclose the channel (Figure 7). The four lysine rings (K200, K209, K234, and K235) are scattered inside the channel and have been proposed to play a role in DNA

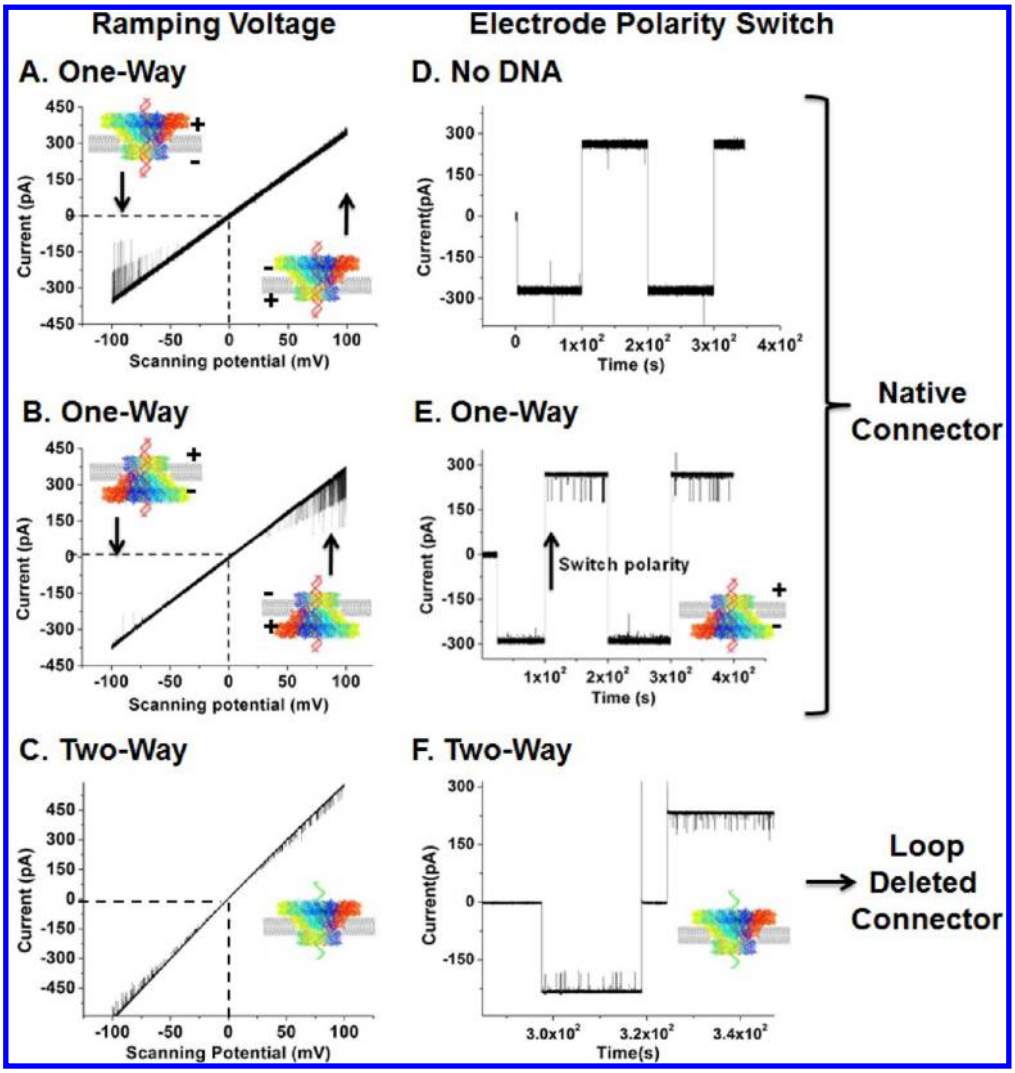

Figure 6. Single-pore conductance assay for DNA translocation through phi29 connector. Unidirectional translocation of dsDNA through wide-type phi29 connector was shown under a ramping potential from −100 mV to +100 mV (A,B) and by switching polarity (E). Single-stranded DNA exhibits a two-way traffic property through internal loop-deleted connector, as shown by ramping potential (C) and by switching polarity (F). (D) Negative control without DNA.

translocation.[33] However, we have found that mutation of one layer of the four lysine rings does not significantly affect motor action.[61]

Here we further investigate the detailed interaction of lysine residues with the bacteriophage genome during translocation. When DNA revolves through the connector, it goes through 12 subunits of the connector per cycle, and we hypothesized that only one strand touches the channel wall. Thus, during the entire 360° revolution, the negatively charged phosphate backbone will be in contact with the same positively charged layer of the lysine ring. One 360° revolution corresponds to 10.5 bp for each helical turn of the B-type dsDNA. This results in an imperfect match (10.5 ÷ 12 = 0.875) of sequential contact between the base, which has the negatively charged DNA phosphate group, and the channel subunits, which contain the positive-charged lysine ring (Figure 7).

On average, each of the four lysine layers will be responsible for contact with three subunits (12 subunits ÷ 4 layers = 3 subunits). This value indicates that, for every three subunits, 2.6 bp (0.875 × 3 = 2.6 bp) will be translocated through the connector. At each step, a 12.5% mismatch occurs (1 − (10.5 ÷ 12)) × 100% = 12.5%. After three transactions with three subunits, a 37.5% variation will occur (12.5% × 3 = 37.5%), and the charge/charge interaction will be weakened due to distance. The phosphate interacts with the optimally charged lysine in the next subunit, and the distance variation due to this mismatch will be compensated for by introducing next lysine layer (Figures 7 and 8). The contact point between the phosphate and the lysine then shifts to the next lysine ring. The transition results in a slight pause during DNA advancement. When dsDNA translocates through three subunits, the heading phosphate of the DNA will have to transition into

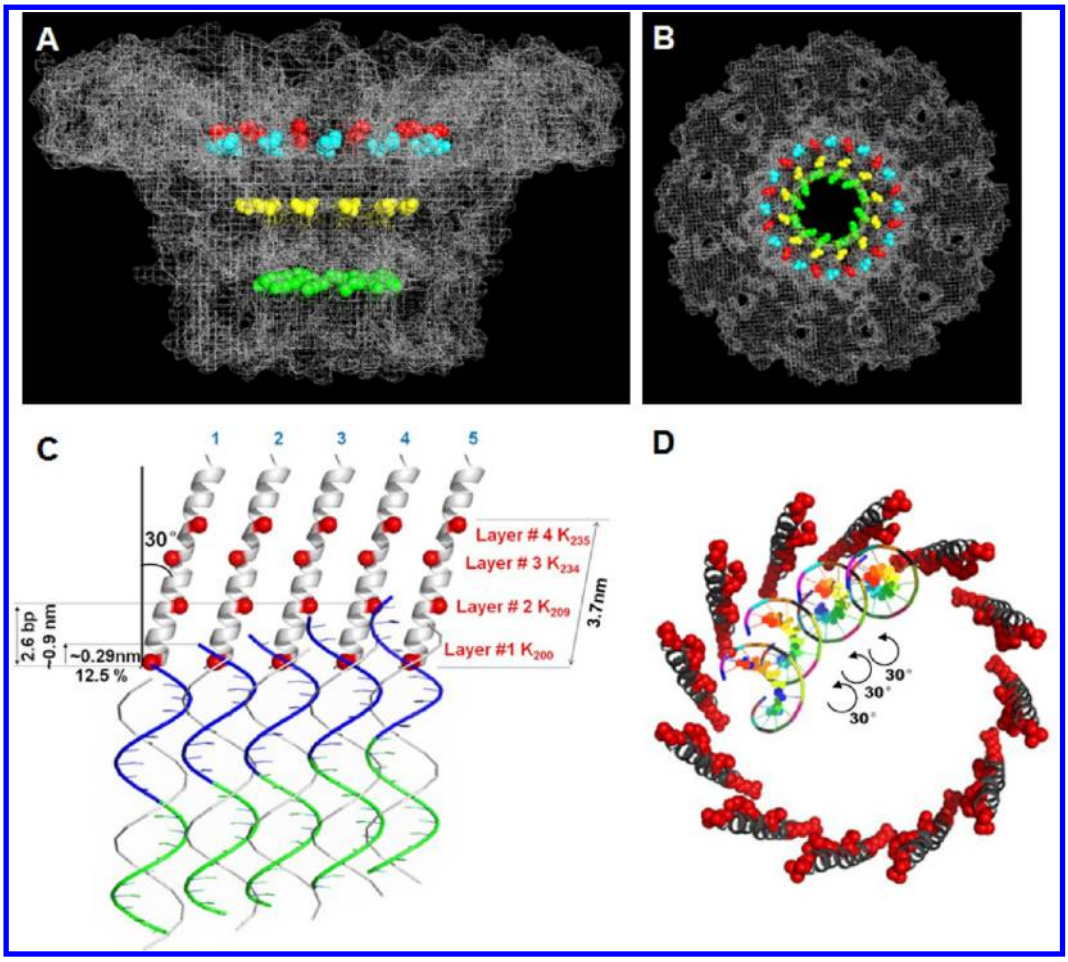

Figure 7. Structure of the phi29 DNA packaging motor, showing the four lysine rings scattered inside the inner wall of the connector. Side view (A) and top view (B) of the connector, showing K200 (magenta) and K209 (yellow). The 229 (cyan) with 246 (red) show the boundary of the connector inner flexible loops that harbor the other two lysines. Due to the flexibility of the loop, the crystal structure of this loop is not available, and the known boundary of the loop was used to show the location. Side (C) and top views (D) of the detailed scheme of DNA revolution through the connector are shown. In this figure, the related position of the dsDNA and the connector subunit are displayed as three-dimensional and viewed at different angles; the position of the dsDNA is different between two channel subunits, even though the DNA itself does not rotate.

the next lysine layer in order to compensate for the imperfect match between the phosphate and each lysine residue during DNA advancement through the connector. Thus, the four layers of the lysine ring will result in four pauses of DNA translocation. We found that the mutation of only one layer of the four lysine rings does not significantly affect motor function,[61] indicating that the interaction of the lysine with the phosphate is only the auxiliary force and not the main force necessary for motor action. This also indicates that the uneven speed of the four-step pauses caused by the four lysine layers is not the essential function of the motor. This would explain why the lysine layer and the 10.5 base per patch are not a perfect match, and why the distance of the layers are not constant.

Based on the crystal structure, the length of the connector channel is ~7 nm. Vertically, these four lysine layers fall within a 3.7 nm[33] range and are spaced approximately ~0.9 nm apart. The lysine residues K234 and K235 lie in the inner loop of the connector between residues 229 to 246, which were missing in the crystal structure; so the two residues close to the boundary of the inner loops were represented and were used to estimate the location (Figure 7). Since B-type dsDNAs have a pitch of 0.34 nm/bp, ~2.6 bp per rise along its axis between two lysine layers can be used in translocation (0.9 nm/0.34 nm·bp^{-1} = ~2.6 bp). This value agrees with the recent data demonstrating the presence of four steps of pauses during the dsDNA translocation process, as measured by optical tweezers using single-molecule analysis.[45,46] It was demonstrated that each step translocated 2.5 base pairs and each circle translocated 10 base pairs of dsDNA.[45,46] The step size is in good agreement with our finding described above. However, the authors interpreted the four pauses caused by four lysine rings into the rotation model driven by four motor ATPase. Thus, they found that their model is in disagreement with both the hexamer[16,23,24,49,60,72,73] and pentamer[74−76] models. Subsequently, the authors

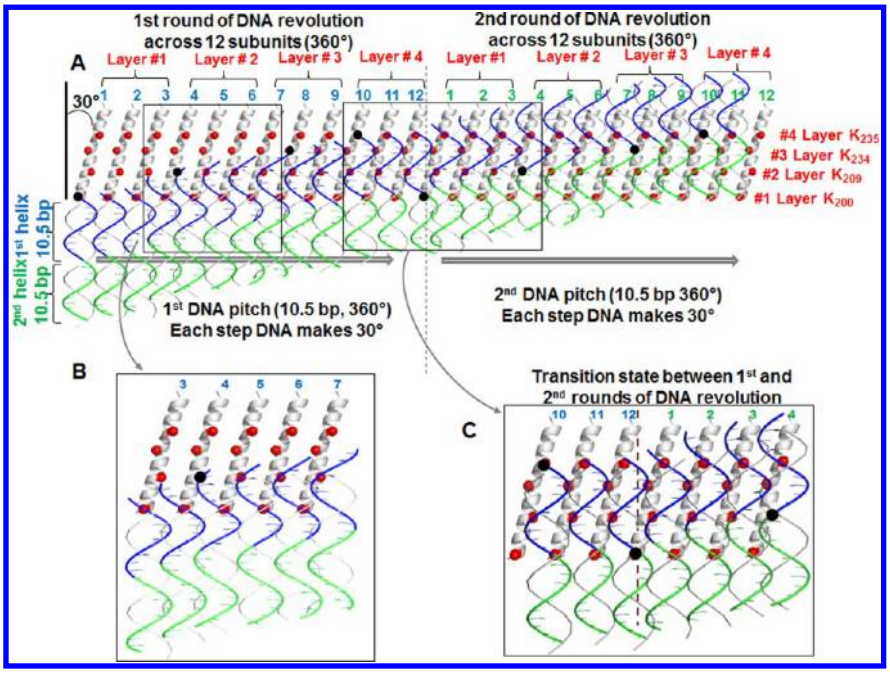

Figure 8. Schematic diagram of DNA revolution inside the phi29 connector channel. (A) Two rounds of DNA revolution across 12 connector subunits. In the first round, a 21 bp DNA helix shown in blue (10.5 bp) and green (10.5 bp) revolves through each subunit, making electrostatic interactions with its negatively charged phosphate group with the positively charged amino group of lysine residues (shown by red spheres in each subunit). The interaction of DNA and lysine is shown by black spheres. During the movement, a DNA strand passes all four lysine layers. The first round ends (blue strand inside the channel) upon DNA making 360° rotation equivalent to 10.5 bp and moving up 1 DNA pitch, ~3.4 nm (subunit #12). This is followed by the second round of rotation. In the same manner, the same DNA strand (green) moves through four lysine layers until the whole helical turn is achieved. The phosphate backbone of the dsDNA contacts the same layer of the lysine every three subunits (12 subunits ÷ 4 layers = 3 subunits/layer) and shifts to the next layer after it revolves through three subunits. (B) Magnified view of DNA at the subunits 3−7 and (C) magnified view of the transition state between two rounds.

proposed a model in which the phi29 DNA packaging motor is a pentamer, but one subunit of the pentamer was inactive, resulting in four motor subunits that generate four power strokes or bursts in rotation. Their rotation model is contradictory to our revolution mechanism described above, showing that the four pauses are due to the presence of four lysine layers in the connector (Figures 7 and 8).[55,56]

MATERIALS AND METHODS

***In Vitro* Virion Assembly Assay.** Purified *in vitro* components were mixed and subjected to the virion assembly assay, as previously described.[70] Briefly, newly assembled infectious virions were inoculated with *Bacillus* bacteria and plated. Activity was expressed as the number of plaques formed per volume of sample (pfu/mL).

Electrophoretic Mobility Shift Assay (EMSA). The fluorescently tagged protein was shown to possess similar assembly and packaging activity as compared to wild-type.[58,62] Cy3-dsDNA (40 bp) was prepared by annealing two complementary DNA oligos containing Cy3 labels (IDT) at their 5′ ends and purifying them with a 10% polyacrylamide gel. Samples were prepared in 20 μL of buffer A (20 mM Tris-HCl, 50 mM NaCl, 1.5% glycerol, 0.1 mM Mg^{2+}). Samples were incubated at ambient temperature for 20 min and then loaded onto a 1% agarose gel (44.5 mM Tris, 44.5 mM boric acid) and electrophoresed at 4 °C for 1 h at 8 V/cm. The eGFP-gp16 and Cy3-DNA samples were analyzed by a fluorescent LightTools Whole Body Imager using 488 and 540 nm excitation wavelengths for GFP and Cy3, respectively.

Single-Pore Conductance Assay for DNA Translocation. The preparation of connector-containing liposomes, the insertion of the connector into the planar bilayer lipid membrane (BLM), and the electrophysiological measurements of DNA through the channel have been described previously.[41,57,77] Briefly, the phi29 connector was inserted into a BLM by vesicle fusion after obtaining connector reconstituted liposomes. A BLM chamber (BCH-1A from Eastern Sci LLC) was used to form horizontal membrane, and a thin Teflon film with an aperture of 70−120 μm (TP-01 from Easter Sci LLC) or 180−250 μm (TP-02) in diameter was used as a partition to separate the chamber into *cis*- and *trans*-compartments. For connector insertions, 1−2 μL of liposome stock solution was diluted by 10−20-fold and was directly added to the *cis*-compartment. A pair of Ag/AgCl electrodes connected directly to the head stage of a current amplifier was used to measure the current across the BLM. The current was recorded by an Axopatch 200B patch clamp amplifier coupled with the Axon DigiData 1322A or Axon DigiData 1440 analog-digital converter (Axon Instruments). All of the electrical signals were obtained from the *trans*-compartment. Data were low band-pass filtered at a frequency of 1 kHz and acquired at 500 μs intervals per signal. The PClamp 9.1 software (Axon Instruments) was used to collect the data, and the software Clampfit was used for data analysis. Conductance measurements were determined using the slope of the current trace induced by a ramp voltage after a definite insertion of a gp10 connector was observed. Solution conductivity was measured using a Pinnacle 542 conductivity/pH meter (Corning Inc.).

Conflict of Interest: The authors declare the following competing financial interest(s): Peixuan Guo is a co-founder of Kylin

Therapeutics and Biomotor and Nucleic Acids Nanotech Development, Ltd.

Acknowledgment. The authors would like to thank Huaming Fang for his work in virion assembly activity assay, and Jeannie Haak for editing this manuscript. The work was supported by NIH Grants R01 EB012135 to P.G., who is a co-founder of Kylin Therapeutics, Inc, and Biomotor and Nucleic Acids Nanotech Development, Ltd.

Supporting Information Available: Animation of DNA revolution through connector. This material is available free of charge *via* the Internet at http://pubs.acs.org.

REFERENCES AND NOTES

1. Kainov, D. E.; Mancini, E. J.; Telenius, J.; Lisai, J.; Grimes, J. M.; Bamford, D. H.; Stuart, D. I.; Tuma, R. Structural Basis of Mechanochemical Coupling in a Hexameric Molecular Motor. *J. Biol. Chem.* **2008**, *283*, 3607–3617.
2. Mastrangelo, I. A.; Hough, P. V.; Wall, J. S.; Dodson, M.; Dean, F. B.; Hurwitz, J. ATP-Dependent Assembly of Double Hexamers of SV40 T Antigen at the Viral Origin of DNA Replication. *Nature* **1989**, *338*, 658–662.
3. Parsons, C. A.; Stasiak, A.; Bennett, R. J.; West, S. C. Structure of a Multisubunit Complex That Promotes DNA Branch Migration. *Nature* **1995**, *374*, 375–378.
4. Egelman, H. H.; Yu, X.; Wild, R.; Hingorani, M. M.; Patel, S. S. Bacteriophage T7 Helicase/Primase Proteins Form Rings around Single-Stranded DNA That Suggest a General Structure for Hexameric Helicases. *Proc. Natl. Acad. Sci. U.S.A.* **1995**, *92*, 3869–3873.
5. Niedenzu, T.; Roleke, D.; Bains, G.; Scherzinger, E.; Saenger, W. Crystal Structure of the Hexameric Replicative Helicase RepA of Plasmid RSF1010. *J. Mol. Biol.* **2001**, *306*, 479–487.
6. Putnam, C. D.; Clancy, S. B.; Tsuruta, H.; Gonzalez, S.; Wetmur, J. G.; Tainer, J. A. Structure and Mechanism of the RuvB Holliday Junction Branch Migration Motor. *J. Mol. Biol.* **2001**, *311*, 297–310.
7. Willows, R. D.; Hansson, A.; Birch, D.; Al-Karadaghi, S.; Hansson, M. EM Single Particle Analysis of the ATP-Dependent BchI Complex of Magnesium Chelatase: An AAA(+) Hexamer. *J. Struct. Biol.* **2004**, *146*, 227–233.
8. Iyer, L. M.; Leipe, D. D.; Koonin, E. V.; Aravind, L. Evolutionary History and Higher Order Classification of AAA Plus ATPases. *J. Struct. Biol.* **2004**, *146*, 11–31.
9. Mueller-Cajar, O.; Stotz, M.; Wendler, P.; Hartl, F. U.; Bracher, A.; Hayer-Hartl, M. Structure and Function of the AAA+ Protein CbbX, a Red-Type Rubisco Activase. *Nature* **2011**, *479*, 194–199.
10. Wang, F.; Mei, Z.; Qi, Y.; Yan, C.; Hu, Q.; Wang, J.; Shi, Y. Structure and Mechanism of the Hexameric MecA-ClpC Molecular Machine. *Nature* **2011**, *471*, 331–335.
11. Grainge, I.; Lesterlin, C.; Sherratt, D. J. Activation of XerCD-Dif Recombination by the FtsK DNA Translocase. *Nucleic Acids Res.* **2011**, *39*, 5140–5148.
12. Martin, A.; Baker, T. A.; Sauer, R. T. Rebuilt AAA + Motors Reveal Operating Principles for ATP-Fuelled Machines. *Nature* **2005**, *437*, 1115–1120.
13. Ammelburg, M.; Frickey, T.; Lupas, A. N. Classification of AAA+ Proteins. *J. Struct. Biol.* **2006**, *156*, 2–11.
14. Guo, P. X.; Lee, T. J. Viral Nanomotors for Packaging of DsDNA and DsRNA. *Mol. Microbiol.* **2007**, *64*, 886–903.
15. Rao, V. B.; Feiss, M. The Bacteriophage DNA Packaging Motor. *Annu. Rev. Genet.* **2008**, *42*, 647–681.
16. Zhang, H.; Schwartz, C.; De Donatis, G. M.; Guo, P. "Push through One-Way Valve" Mechanism of Viral DNA Packaging. *Adv. Virus Res.* **2012**, *83*, 415–465.
17. Serwer, P. A Hypothesis for Bacteriophage DNA Packaging Motors. *Viruses* **2010**, *2*, 1821–1843.
18. Guo, P.; Peterson, C.; Anderson, D. Prohead and DNA-Gp3-Dependent ATPase Activity of the DNA Packaging Protein Gp16 of Bacteriophage Φ29. *J. Mol. Biol.* **1987**, *197*, 229–236.
19. Chemla, Y. R.; Aathavan, K.; Michaelis, J.; Grimes, S.; Jardine, P. J.; Anderson, D. L.; Bustamante, C. Mechanism of Force Generation of a Viral DNA Packaging Motor. *Cell* **2005**, *122*, 683–692.
20. Hwang, Y.; Catalano, C. E.; Feiss, M. Kinetic and Mutational Dissection of the Two ATPase Activities of Terminase, the DNA Packaging Enzyme of Bacteriophage Lambda. *Biochemistry* **1996**, *35*, 2796–2803.
21. Sabanayagam, C. R.; Oram, M.; Lakowicz, J. R.; Black, L. W. Viral DNA Packaging Studied by Fluorescence Correlation Spectroscopy. *Biophys. J.* **2007**, *93*, L17–L19.
22. Guo, P.; Erickson, S.; Anderson, D. A Small Viral RNA Is Required for *In Vitro* Packaging of Bacteriophage Phi29 DNA. *Science* **1987**, *236*, 690–694.
23. Guo, P.; Zhang, C.; Chen, C.; Trottier, M.; Garver, K. Inter-RNA Interaction of Phage Phi29 PRNA To Form a Hexameric Complex for Viral DNA Transportation. *Mol. Cell* **1998**, *2*, 149–155.
24. Shu, D.; Zhang, H.; Jin, J.; Guo, P. Counting of Six PRNAs of Phi29 DNA-Packaging Motor with Customized Single Molecule Dual-View System. *EMBO J.* **2007**, *26*, 527–537.
25. Guo, P.; Peterson, C.; Anderson, D. Initiation Events in *In Vitro* Packaging of Bacteriophage Φ29 DNA-Gp3. *J. Mol. Biol.* **1987**, *197*, 219–228.
26. Huang, L. P.; Guo, P. Use of Acetone To Attain Highly Active and Soluble DNA Packaging Protein Gp16 of Phi29 for ATPase Assay. *Virology* **2003**, *312*, 449–457.
27. Huang, L. P.; Guo, P. Use of PEG To Acquire Highly Soluble DNA-Packaging Enzyme Gp16 of Bacterial Virus Phi29 for Stoichiometry Quantification. *J. Virol. Methods* **2003**, *109*, 235–244.
28. Lee, T. J.; Guo, P. Interaction of Gp16 with PRNA and DNA for Genome Packaging by the Motor of Bacterial Virus Phi29. *J. Mol. Biol.* **2006**, *356*, 589–599.
29. Lee, T. J.; Zhang, H.; Liang, D.; Guo, P. Strand and Nucleotide-Dependent ATPase Activity of Gp16 of Bacterial Virus Phi29 DNA Packaging Motor. *Virology* **2008**, *380*, 69–74.
30. Ibarra, B.; Valpuesta, J. M.; Carrascosa, J. L. Purification and Functional Characterization of P16, the ATPase of the Bacteriophage Phi29 Packaging Machinary. *Nucleic Acids Res.* **2001**, *29*, 4264–4273.
31. Grimes, S.; Anderson, D. RNA Dependence of the Bateriophage Phi29 DNA Packaging ATPase. *J. Mol. Biol.* **1990**, *215*, 559–566.
32. Jimenez, J.; Santisteban, A.; Carazo, J. M.; Carrascosa, J. L. Computer Graphic Display Method for Visualizing Three-Dimensional Biological Structures. *Science* **1986**, *232*, 1113–1115.
33. Guasch, A.; Pous, J.; Ibarra, B.; Gomis-Ruth, F. X.; Valpuesta, J. M.; Sousa, N.; Carrascosa, J. L.; Coll, M. Detailed Architecture of a DNA Translocating Machine: The High-Resolution Structure of the Bacteriophage Phi29 Connector Particle. *J. Mol. Biol.* **2002**, *315*, 663–676.
34. Green, D. J.; Wang, J. C.; Xiao, F.; Cai, Y.; Balhorn, R.; Guo, P.; Cheng, R. H. Self-Assembly of Heptameric Nanoparticles Derived from Tag-Functionalized Phi29 Connectors. *ACS Nano* **2010**, *4*, 7651–7659.
35. Xiao, F.; Cai, Y.; Wang, J. C.; Green, D.; Cheng, R. H.; Demeler, B.; Guo, P. Adjustable Ellipsoid Nanoparticles Assembled from Re-engineered Connectors of the Bacteriophage Phi29 DNA Packaging Motor. *ACS Nano* **2009**, *3*, 2163–2170.
36. Xiao, F.; Demeler, B.; Guo, P. Assembly Mechanism of the Sixty-Subunit Nanoparticles *via* Interaction of RNA with the Reengineered Protein Connector of Phi29 DNA-Packaging Motor. *ACS Nano* **2010**, *4*, 3293–3301.
37. Guo, Y.; Blocker, F.; Xiao, F.; Guo, P. Construction and 3-D Computer Modeling of Connector Arrays with Tetragonal to Decagonal Transition Induced by PRNA of Phi29 DNA-Packaging Motor. *J. Nanosci. Nanotechnol.* **2005**, *5*, 856–863.
38. Carazo, J. M.; Donate, L. E.; Herranz, L.; Secilla, J. P.; Carrascosa, J. L. Three-Dimensional Reconstruction of the Connector of Bacteriophage Φ29 at 1.8 nm Resolution. *J. Mol. Biol.* **1986**, *192*, 853–867.
39. Xiao, F.; Sun, J.; Coban, O.; Schoen, P.; Wang, J. C.; Cheng, R. H.; Guo, P. Fabrication of Massive Sheets of Single Layer

Patterned Arrays Using Lipid Directed Reengineered Phi29 Motor Dodecamer. *ACS Nano* **2009**, *3*, 100–107.
40. Haque, F.; Lunn, J.; Fang, H.; Smithrud, D.; Guo, P. Real-Time Sensing and Discrimination of Single Chemicals Using the Channel of Phi29 DNA Packaging Nanomotor. *ACS Nano* **2012**, *6*, 3251–3261.
41. Wendell, D.; Jing, P.; Geng, J.; Subramaniam, V.; Lee, T. J.; Montemagno, C.; Guo, P. Translocation of Double-Stranded DNA through Membrane-Adapted Phi29 Motor Protein Nanopores. *Nat. Nanotechnol.* **2009**, *4*, 765–772.
42. Hendrix, R. W. Symmetry Mismatch and DNA Packaging in Large Bacteriophages. *Proc. Natl. Acad. Sci. U.S.A.* **1978**, *75*, 4779–4783.
43. Doering, C.; Ermentrout, B.; Oster, G. Rotary DNA Motors. *Biophys. J.* **1998**, *69*, 2256–2267.
44. Maluf, N. K.; Gaussier, H.; Bogner, E.; Feiss, M.; Catalano, C. E. Assembly of Bacteriophage Lambda Terminase into a Viral DNA Maturation and Packaging Machine. *Biochemistry* **2006**, *45*, 15259–15268.
45. Yu, J.; Moffitt, J.; Hetherington, C. L.; Bustamante, C.; Oster, G. Mechanochemistry of a Viral DNA Packaging Motor. *J. Mol. Biol.* **2010**, *400*, 186–203.
46. Moffitt, J. R.; Chemla, Y. R.; Aathavan, K.; Grimes, S.; Jardine, P. J.; Anderson, D. L.; Bustamante, C. Intersubunit Coordination in a Homomeric Ring ATPase. *Nature* **2009**, *457*, 446–450.
47. Aathavan, K.; Politzer, A. T.; Kaplan, A.; Moffitt, J. R.; Chemla, Y. R.; Grimes, S.; Jardine, P. J.; Anderson, D. L.; Bustamante, C. Substrate Interactions and Promiscuity in a Viral DNA Packaging Motor. *Nature* **2009**, *461*, 669–673.
48. Guo, P.; Grimes, S.; Anderson, D. A Defined System for *In Vitro* Packaging of DNA-Gp3 of the *Bacillus subtilis* Bacteriophage Phi29. *Proc. Natl. Acad. Sci. U.S.A.* **1986**, *83*, 3505–3509.
49. Zhang, F.; Lemieux, S.; Wu, X.; St.-Arnaud, S.; McMurray, C. T.; Major, F.; Anderson, D. Function of Hexameric RNA in Packaging of Bacteriophage Phi29 DNA *in Vitro*. *Mol. Cell* **1998**, *2*, 141–147.
50. Hendrix, R. W. Bacteriophage DNA Packaging: RNA Gears in a DNA Transport Machine (Minireview). *Cell* **1998**, *94*, 147–150.
51. Baumann, R. G.; Mullaney, J.; Black, L. W. Portal Fusion Protein Constraints on Function in DNA Packaging of Bacteriophage T4. *Mol. Microbiol.* **2006**, *61*, 16–32.
52. Hugel, T.; Michaelis, J.; Hetherington, C. L.; Jardine, P. J.; Grimes, S.; Walter, J. M.; Faik, W.; Anderson, D. L.; Bustamante, C. Experimental Test of Connector Rotation during DNA Packaging into Bacteriophage Phi29 Capsids. *PLoS Biol.* **2007**, *5*, 558–567.
53. Chang, C.; Zhang, H.; Shu, D.; Guo, P.; Savran, C. Bright-Field Analysis of Phi29 DNA Packaging Motor Using a Magnetomechanical System. *Appl. Phys. Lett.* **2008**, *93*, 153902–153902-3.
54. Maluf, N. K.; Feiss, M. Virus DNA Translocation: Progress towards a First Ascent of Mount Pretty Difficult. *Mol. Microbiol.* **2006**, *61*, 1–4.
55. Schwartz, C.; De Donatis, G. M.; Zhang, H.; Fang, H.; Guo, P. Revolution Rather than Rotation of AAA+ Hexameric Phi29 Nanomotor for Viral DsDNA Packaging without Coiling. *Virology* **2013**, Manuscript in preparation.
56. Schwartz, C.; De Donatis, G. M.; Fang, H.; Guo, P. The ATPase of the Phi29 DNA-Packaging Motor Is a Member of the Hexameric AAA+ Superfamily. *Virology* **2013**, Manuscript in preparation.
57. Jing, P.; Haque, F.; Shu, D.; Montemagno, C.; Guo, P. One-Way Traffic of a Viral Motor Channel for Double-Stranded DNA Translocation. *Nano Lett.* **2010**, *10*, 3620–3627.
58. Lee, T. J.; Zhang, H.; Chang, C. L.; Savran, C.; Guo, P. Engineering of the Fluorescent-Energy-Conversion Arm of Phi29 DNA Packaging Motor for Single-Molecule Studies. *Small* **2009**, *5*, 2453–2459.
59. Shu, Y.; Haque, F.; Shu, D.; Li, W.; Zhu, Z.; Kotb, M.; Lyubchenko, Y.; Guo, P. Fabrication of 14 Different RNA Nanoparticles for Specific Tumor Targeting without Accumulation in Normal Organs. *RNA* **2013**, in press.
60. Zhang, H.; Endrizzi, J. A.; Shu, Y.; Haque, F.; Guo, P.; Chi, Y. I. The 3WJ Core Crystal Structure Reveals Divalent Ion-Promoted Thermostability and Functional Assembly of the Phi29 Hexameric Motor PRNA. *RNA* **2012**Submitted.
61. Fang, H.; Jing, P.; Haque, F.; Guo, P. Role of Channel Lysines and "Push through a One-Way Valve" Mechanism of Viral DNA Packaging Motor. *Biophys. J.* **2012**, *102*, 127–135.
62. Schwartz, C.; Fang, H.; Huang, L.; Guo, P. Sequential Action of ATPase, ATP, ADP, Pi and DsDNA in Procapsid-Free System To Enlighten Mechanism in Viral DsDNA Packaging. *Nucleic Acids Res.* **2012**, *40*, 2577–2586.
63. Morita, M.; Tasaka, M.; Fujisawa, H. DNA Packaging ATPase of Bacteriophage T3. *Virology* **1993**, *193*, 748–752.
64. Geng, J.; Fang, H.; Haque, F.; Zhang, L.; Guo, P. Three Reversible and Controllable Discrete Steps of Channel Gating of a Viral DNA Packaging Motor. *Biomaterials* **2011**, *32*, 8234–8242.
65. Grimes, S.; Ma, S.; Gao, J.; Atz, R.; Jardine, P. J. Role of Phi29 Connector Channel Loops in Late-Stage DNA Packaging. *J. Mol. Biol.* **2011**, *410*, 50–59.
66. Isidro, A.; Henriques, A. O.; Tavares, P. The Portal Protein Plays Essential Roles at Different Steps of the SPP1 DNA Packaging Process. *Virology* **2004**, *322*, 253–263.
67. Geng, J.; Huaming, F.; shaoying, W.; Peixuan, G. Channel Size Conversion of Phi29 DNA-Packaging Nanomotor for Discrimination of Single- and Double-Stranded DNA and RNA. *ACS Nano* **2013**, 10.1021/nn400020z.
68. Moll, W.-D.; Guo, P. Translocation of Nicked but Not Gapped DNA by the Packaging Motor of Bacteriophage Phi29. *J. Mol. Biol.* **2005**, *351*, 100–107.
69. Lee, C. S.; Guo, P. *In Vitro* Assembly of Infectious Virions of Ds-DNA Phage Φ29 from Cloned Gene Products and Synthetic Nucleic Acids. *J. Virol.* **1995**, *69*, 5018–5023.
70. Lee, C. S.; Guo, P. A Highly Sensitive System for the Assay of *In Vitro* Viral Assembly of Bacteriophage Phi29 of *Bacillus subtilis*. *Virology* **1994**, *202*, 1039–1042.
71. Oram, M.; Sabanayagam, C.; Black, L. W. Modulation of the Packaging Reaction of Bacteriophage T4 Terminase by DNA Structure. *J. Mol. Biol.* **2008**, *381*, 61–72.
72. Xiao, F.; Zhang, H.; Guo, P. Novel Mechanism of Hexamer Ring Assembly in Protein/RNA Interactions Revealed by Single Molecule Imaging. *Nucleic Acids Res.* **2008**, *36*, 6620–6632.
73. Ibarra, B.; Caston, J. R.; Llorca, O.; Valle, M.; Valpuesta, J. M.; Carrascosa, J. L. Topology of the Components of the DNA Packaging Machinery in the Phage Phi29 Prohead. *J. Mol. Biol.* **2000**, *298*, 807–815.
74. Morais, M. C.; Koti, J. S.; Bowman, V. D.; Reyes-Aldrete, E.; Anderson, D.; Rossman, M. G. Defining Molecular and Domain Boundaries in the Bacteriophage Phi29 DNA Packaging Motor. *Structure* **2008**, *16*, 1267–1274.
75. Morais, M. C.; Tao, Y.; Olsen, N. H.; Grimes, S.; Jardine, P. J.; Anderson, D.; Baker, T. S.; Rossmann, M. G. Cryoelectron-Microscopy Image Reconstruction of Symmetry Mismatches in Bacteriophage Phi29. *J. Struct. Biol.* **2001**, *135*, 38–46.
76. Ding, F.; Lu, C.; Zhao, W.; Rajashankar, K. R.; Anderson, D. L.; Jardine, P. J.; Grimes, S.; Ke, A. Structure and Assembly of the Essential RNA Ring Component of a Viral DNA Packaging Motor. *Proc. Natl. Acad. Sci. U.S.A.* **2011**, *108*, 7357–7362.
77. Jing, P.; Haque, F.; Vonderheide, A.; Montemagno, C.; Guo, P. Robust Properties of Membrane-Embedded Connector Channel of Bacterial Virus Phi29 DNA Packaging Motor. *Mol. BioSyst.* **2010**, *6*, 1844–1852.